Phytochemistry 222 (2024) 114075

Contents lists available at ScienceDirect

Phytochemistry

journal homepage: www.elsevier.com/locate/phytochem

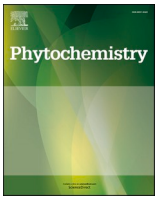

Insecticidal bisindole alkaloids from leaves of *Tabernaemontana divaricata* 'Dwaft'

Jing Chen [a], Sumet Kongkiatpaiboon [b,**], Xiang-Hai Cai [a,*]

[a] State Key Laboratory of Phytochemistry and Plant Resources in West China, Kunming Institute of Botany, Chinese Academy of Sciences, Kunming, 650201, China
[b] Drug Discovery and Development Center, Office of Advanced Science and Technology, Thammasat University, Pathum Thani, 12121, Thailand

ARTICLE INFO

Keywords:
Apocynaceae
Tabernaemontana divaricata 'Dwaft'
Bisindole alkaloids
Strychnos–iboga type
Aspidosperma–iboga type
Insecticide

ABSTRACT

Six undescribed bisindole alkaloids, namely taberdisines A–F (**1**–**6**), were isolated from the leaves of *Tabernaemontana divaricata* 'Dwaft'. Among them, alkaloids **1** and **2** were the first examples of strychnos–iboga type alkaloid with both C–C linkage patterns. Alkaloid **3**, a new type of aspidosperma–iboga with a furan-ring, as well as other three undescribed ones was disclosed. Their structures were elucidated by comprehensive spectroscopic analyses. Alkaloids **1** and **5** showed insecticide activity on *Sf9* cell and eggs of *Spodoptera frugiperda* in vivo, which might explain the potential of the plants for insect resistance.

1. Introduction

Tabernaemontana Linn. plants of family Apocynaceae, including approximate 120 species, are naturally distributed in tropical area. This genus is often found to free from insect infestation, indicating the presence of potential insect resistance. According to research findings, different kinds of compounds, such as essential oils, terpenoids, alkaloids, and phenolic, act as larvicides, ovicides, mosquito repellents, and potent insecticides (Duke et al., 2019; Hillary et al., 2024). At present, more than 2000 species of plants have been reported to produce secondary metabolites with anti-insect activity (Ganesan et al., 2023). Among them, some scientists have also explored the insecticidal activity components of *Tabernaemontana* genus and made some important discoveries. For example, the beetles expressed strong repellent behavior against the acetone extracts of leaves of *T. divaricata* (Dwivedi and Venugopalan, 2002). The extract of *T. coronaria* was also shown to have larvicidal effects on mosquitoes (Mathivanan et al., 2013). The crude extract of *T. coronaria* exerted zero hatchability at 150 ppm for *Culex quinquefasciatus, Aedes aegypti* and *Anppheles stephensi,* respectively (Govindarajan et al., 2011a,b). Benzene extract of *T. coronaria* exhibited excellent mortality against early third instar of *Anopheles subpictus* and had an excellent killing effect on the larvae of three other mosquito species (Govindarajan et al., 2011, 2012). The hydroethanolic extract of *T. elegans* (leaves) caused a very high mortality rate in *Rhipicephalus turanicus* (Fouche et al., 2019). However, we notice that most of these findings were at the crude extract level, and the core monomer components still have not been discovered. These findings attracted us to further investigate the special components of the *Tabernaemontana* genus.

T. divaricata 'Dwaft', as a cultivated variety of *T. divaricata*, are widely cultivated as ornamental plant in Southeast Asia. Based on our previous explore the effects of artificial planting and habitat on plants (Chen et al., 2021), we continue conducted the systematic study on samples of this plant collected from Bangkok, Thailand. Interestingly, in addition to the previously reported active structures, six novel bisindole alkaloids with anti-insect activity were disclosed by bioactive screening (Fig. 1). The occurrence of these bioactive compounds in the leaves suggested the function as defense chemicals against overground organisms.

2. Results and discussion

Compound **1** was obtained as amorphous pale powder, and its molecular formula was determined to be $C_{40}H_{46}N_4O_4$ by high resolution electrospray ionization mass spectrometry (HRESIMS) based on the ion at *m/z* 647.3594 $[M+H]^+$ (calcd. for $C_{40}H_{47}N_4O_4$ 647.3592), indicating 20 degrees of unsaturation. The UV absorption bands at 206, 221 and 298 nm of **1** were the characteristic of an indole chromophore (Albinsson and Norden, 1992). The ^{13}C NMR spectrum of **1** (Table 1) contained 40 resonances, attributable to two carbonyls, two methyls, two

* Corresponding author.
** Corresponding author.
E-mail addresses: sumet_k@tu.ac.th (S. Kongkiatpaiboon), xhcai@mail.kib.ac.cn (X.-H. Cai).

https://doi.org/10.1016/j.phytochem.2024.114075
Received 16 November 2023; Received in revised form 26 March 2024; Accepted 26 March 2024
Available online 1 April 2024

methoxys, one sp^2 and nine sp^3 methylenes, 11 methines, and 12 sp^2 and one sp^3quaternary carbons. The ^1H and ^{13}C NMR spectrum of **1** (Tables 1 and 2) displayed two singlets of indolic NH at δ_H 10.42 and 9.06, an unsubstituted indole A-ring (unit A), and an *ortho*-disubstituted indole A-ring (unit B). Above NMR data indicated **1** as a bisindole in agreement with the HRESIMS. As for unit A, there were four unsubstituted indole protons (δ_H 7.40, 7.29, 7.11, 6.93) and a pair of singlets at δ_H 5.27 and 4.98 of exocyclic double bond (CH_2-22), resembles to the strychnos–type alkaloids that take apparicine (van Beek et al., 1984), pericine (Arens et al., 1982; Kobayashi et al., 2002), and pericidine (Lim and Kam, 2007) as examples. Further careful comparison of the NMR spectrum with the above known alkaloids revealed presence of apparicine analogue unit in **1** with exception for some differences. Like pericidine (Lim and Kam, 2007), the HMBC correlations of δ_H 1.72 (d, $J = 7.2$ Hz, H-18) and δ_H 7.03 (q, $J = 7.2$ Hz, H-19) with δ_C 165.0 (C-21) placed the carbonyl group at C-21. Another conspicuous difference between **1** and apparicine was the sharply upfielded signal of C-6 (δ_C 45.3 in apparicine; δ_C 25.6 in **1**) (Table 1). This suggested that a cleavage occurred between C-6 and N-4. Unit B showed similar resonances to those of voacangine (Sharma and Cordell, 1988), which displayed the iboga fragment. The HMBC cross-peak (Fig. 2) of δ_H 6.98 to δ_C 110.2 (C-7′) assigned the singlet hydrogen as H-9'. Similarly, the other singlet δ_H 6.55 was elucidated as H-12′ by cross-peak of δ_H 6.55/C-7. 10′-OMe was located by the HMBC correlations of both H-12′ and OCH_3 with δ_C 152.7 (C-10′). C-11′ substitution could be confirmed by NH' (δ_H 9.06) and the aromatic protons (δ_H 6.55) to the indole ring carbons, δ_C 127.8 (C-8′), 152.7 (C-10′), 125.6 (C-11′), and 131.7 (C-13′), together with the aromatic methoxy group at δ_H 3.93 to δ_C 152.7(C-10′).

The HMBC cross-peaks (Fig. 2) of H-6 (δ_H 4.21, q, $J = 17.3$ Hz) with δ_C 152.7 (C-10′), 125.6 (C-11′), 111.5 (C-12′), 131.7 (C-13′), 136.2 (C-2) and 130.3 (C-8) confirmed the linkage between C-6 and C-11'. The ROESY correlations (Fig. 2) of H-18 with NH, H-15, NH' and H-12′ confirmed the α-orientation of H-15 which was in agreement with that of the reported apparicine. Meanwhile, the ROESY correlations of H-20′ with H-21′, H-18′ and $COOCH_3$' also suggested the relative configurations of iboga unit was also the same as voacangine. Therefore, the structure of compound **1** was elucidated and named as taberdisine A. To our best knowledge, it was the first case of strychnos–iboga bisindole alkaloid connected by single carbon bond.

The UV spectrum of compound **2** showed close similarity to that of **1**. The molecular formula displayed as $C_{40}H_{46}N_4O_5$ based on its HRESIMS data at *m/z* 663.3543 $[M + H]^+$ (calcd for $C_{40}H_{47}N_4O_5$ 663.3541), 16 Da more than that of **1**. A direct comparison of the NMR spectra of **1** and **2** (Tables 1 and 2) indicated that both compounds shared the same basic skeleton as the strychnos–iboga type bisindole alkaloid. The only difference arose from an additional hydroxyl group substituted at C-19′ in iboga unit in **2**. This was conspicuously demonstrated by the downfield shift of the carbon resonances at position C-18' (δ_C from 11.9 in **1** to 21.0 in **2**) and 19' (from δ_C 27.8 in **1** to 71.5 in **2**) compared with **1**. The HMBC correlations from δ_H 0.98 (d, $J = 6.4$ Hz, H-18′) to δ_C 71.5 (C-19′) could supported it.

Due to the close spatial distance, it was difficult to confirm the configuration of C-19′ by the ROESY signals. However, there was a characteristics of the NMR data in this Iboga–type alkaloid with 19′-OH that the chemical shift of C-15/21 resonated at δ_C 23 and 60 in 19′*S*-configuration, while δ_C 29 and 54 in the 19′*R*-configuration (Gunasekera et al., 1980; Perera et al., 1983; Kam and Sim, 2002; Kam et al., 1998; Chaturvedula et al., 2003). Therefore, the configuration of the C-19′ was determined to be *S* by its carbon shifts of δ_C 24.5 (C-15′) and δ_C 60.5 (C-21′). Thus **2** was subsequently named taberdisine B.

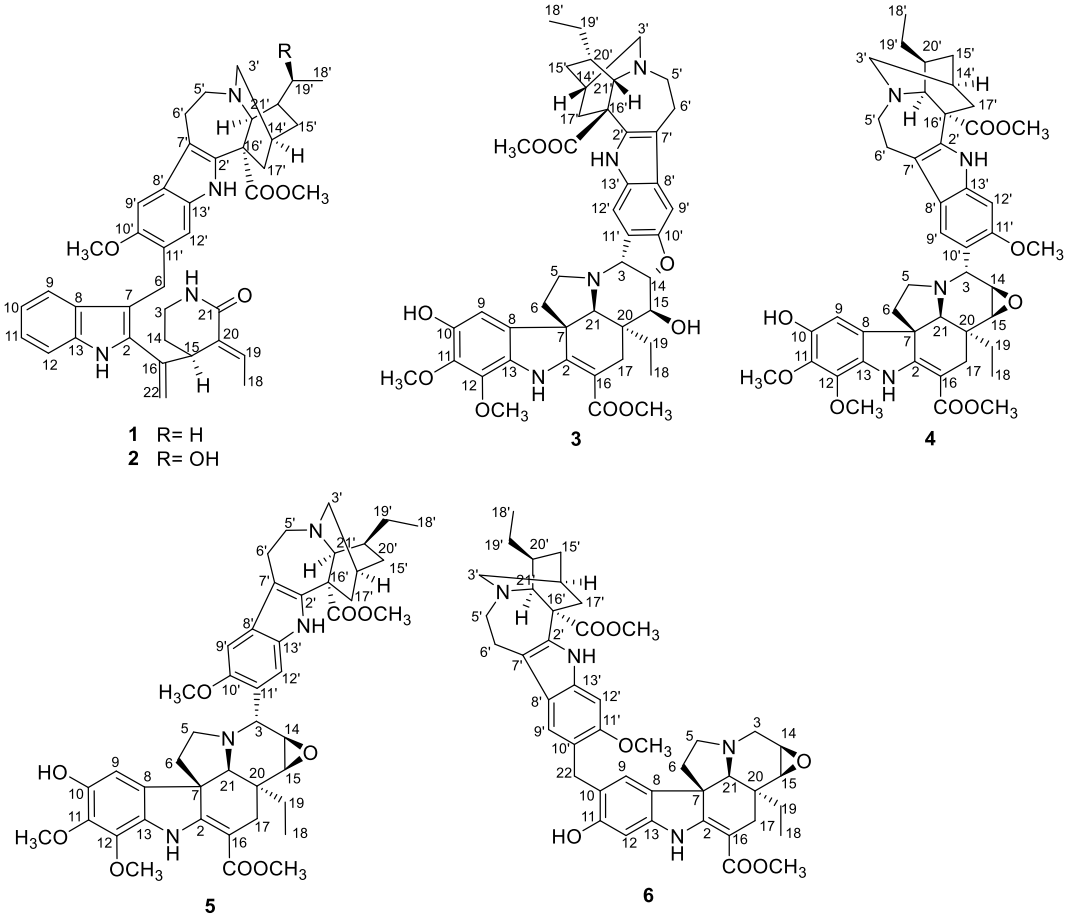

Fig. 1. Structures of bisindole alkaloids **1**–**6**.

Table 1
^{13}C NMR spectroscopic data of alkaloids **1**–**3** in acetone-d_6 (δ in ppm and J in Hz, 150 MHz).

No.	1[a]		2[a]		3[a]	
	unit A	unit B	unit A	unit B	unit A	unit B
2/2′	136.2 C	138.3 C	136.2 C	137.1 C	165.6 C	139.9 C
3/3′	38.4 CH_2	52.8 CH_2	38.3 CH_2	52.3 CH_2	60.7 CH	52.7 CH_2
5/5′		54.3 CH_2		53.4 CH_2	46.6 CH_2	54.1 CH_2
6/6′	25.6 CH_2	22.7 CH_2	25.6 CH_2	22.2 CH_2	42.4 CH_2	22.7 CH_2
7/7′	112.6 C	110.2 C	112.5 C	109.8 C	55.8 C	110.0 C
8/8′	130.3 C	127.8 C	130.3 C	127.6 C	134.5 C	132.7 C
9/9′	120.0 CH	99.2 CH	120.0 CH	99.2 CH	106.5 CH	109.1 CH
10/10′	119.8 CH	152.7 C	119.9 CH	152.8 C	145.6 C	119.3 C
11/11′	122.7 C	125.6 C	122.7 C	126.0 C	140.3 C	155.3 C
12/12′	111.8 C	111.5 CH	111.8 C	111.5 CH	137.9 C	97.5 CH
13/13′	137.1 C	131.7 C	137.6 C	131.8 C	128.9 C	131.0 C
14/14′	27.2 CH_2	28.2 CH	27.2 CH_2	27.7 CH	85.1 CH	28.2 CH
15/15′	39.2 CH	32.8 CH_2	39.2 CH	24.5 CH_2	70.5 CH	32.9 CH_2
16/16′	140.5 C	55.9 C	140.5 C	55.2 C	91.4 C	56.0 C
17/17′		37.0 CH_2		37.4CH_2	23.1 CH_2	36.8 CH_2
18/18′	13.3 CH_3	11.9 CH_3	13.3 CH_3	21.0 CH_3	7.8 CH_3	11.9 CH_3
19/19′	135.5 CH	27.8 CH_2	135.5 CH	71.5 CH	27.4 CH_2	27.7 CH_2
20/20′	132.1 C	39.5 CH	132.1 C	41.2CH	45.8 C	39.5 CH
21/21′	165.0 C	58.1 CH	165.0 C	60.5 CH	66.0 CH	58.1 CH
22	117.2 CH_2		117.2 CH_2			
$\underline{COOCH_3}$		175.1 C		174.6 C	169.1 C	175.4 C
$COO\underline{CH_3}$		52.5 CH_3		52.7 CH_3	50.9 CH_3	52.6 CH_3
10-OCH_3						
11-OCH_3		56.0 CH_3		56.0 CH_3		
11′-OCH_3					61.0 CH_3	
12′-OCH_3					60.7 CH_3	

Compound **3** possessed a molecular formula of $C_{44}H_{52}N_4O_9$ deduced by a HRESIMS ion peak at m/z 781.3803 $[M + H]^+$ (calcd. for $C_{44}H_{53}N_4O_9$ 781.3807). The UV absorption of **3** bands at 204, 219, 304 and 336 nm suggested the presence of β-anilinoacrylate chromophores (Kam et al., 2003). The ^{13}C NMR spectrum (Table 1) contained 44 resonances, attributable to two ester carbonyls, two methyls, four methoxyls, ten methylenes, three sp^2 and seven sp^3 methines, and ten sp^2 and three sp^3 quaternary carbons. The ^{1}H NMR spectrum of **3** (Table 2) displayed two singlets of NH at δ_H 9.35 and 8.75, and two methyls at δ_H 0.90 and 0.71, three aromatic singlets at δ_H 7.48, 6.78 and 5.55. These data indicated that compound **3** was a bisindole. Examination of the ^{13}C NMR spectrum of **3** revealed the 10-hydroxy-11,12-dimethoxytabersonine -β-epoxide unit that occurred in conophylline (Kam et al., 1993). The other iboga unit was similar to isovoacangine (Agwada et al., 1975) with exception for different signals in indole ring A indicated the conjunction position. The C-10′ substitution was present based on the HMBC correlations (Fig. 3) from the aromatic protons δ_H 7.48 (H-12′) to the indole ring carbons δ_C 155.3(C-10′) and 131.0 (C-13′), δ_H 6.55 (H-9′) to δ_C 110.0 (C-7′), 132.7 (C-8′) and 119.3 (C-11′). And the HMBC cross-peaks from δ_H 7.48 (H-12′) to δ_C 60.7 (C-3), δ_H 5.01 (d, J = 7.9 Hz, H-3) to δ_C 85.1 (C-14), 109.1 (C-12′), 119.3 (C-10′), and 155.3 (C-10′), and from δ_H 4.97 (H-14) to δ_C 70.5 (C-15) indicated two coupling units by forming a furan ring through C3–C11′-C10′-O-C14. Interestingly, this formation mode was different from the link order that

Table 2
^{1}H NMR spectroscopic data of alkaloids **1**–**6** in acetone-d_6 (δ in ppm and J in Hz).

No.	1[a]	2[a]	3[a]	4[b]	5[a]	6[a]
NH	10.42, s	10.42, s	8.75, s	8.81, s	8.80, s	9.17, s
3	3.19, m 3.00, m	3.20, m 3.01, m	5.01, d, 7.9	5.01, s	5.06, s	3.40, m 2.85, *
5			3.10, m 2H	3.11, * 2.76, *	3.07, m 2.72, m	2.88, * 2.67, m
6	4.21, q, 17.3 2H	4.21, q, 17.3 2H	2.01, m 1.58, m	1.96, m 1.60, dd, 11.8, 5.2	1.91, m 1.55, *	1.89, m 1.57, m
9	7.29, d, 7.9	7.29, d, 7.9	5.55, s	6.02, s	5.90, s	7.08, s
10	6.93, t, 7.9	6.95, t, 7.9				
11	7.11, t, 7.9	7.11, t, 7.9				
12	7.40, d, 7.9	7.40, d, 7.9				6.58, s
14	1.75, * 2H	1.76, * 2H	4.97, dd, 7.9, 3.5	3.42, d, 3.7	3.28, d, 3.8	3.14, d, 3.7
15	4.27, br s	4.27, br s	4.07, d, 3.5	3.27, d, 3.7	3.20, d, 3.8	2.94, d, 3.7
17			2.68, * 2.54, m	2.66, d, 15.3 2.60, d, 15.3	2.60, m 2H	2.53, m 2H
18	1.72, d, 7.2	1.72, d, 7.2	0.71, t, 7.1	0.83, t, 7.4	0.79, t, 7.2	0.70, t, 7.4
19	7.03, q, 7.2	7.03, q, 7.2	1.23, m 0.78, m	1.16, m 1.00, m	1.11, m 0.94, m	1.22, m 0.77, m
21			2.57, s	3.03, s	2.95, s	2.41, s
22	5.27, s 4.98, s	5.27, s 4.97, s				3.92, * 2H
$COOCH_3$			3.74, s	3.75, s	3.73, s	3.68, s
11′-OCH_3			3.70, s	3.76, s	3.72, s	
12′-OCH_3			3.86, s	3.91, s	3.87, s	
NH’	9.06, s	9.10, s	9.35, s	9.31, s	9.39, s	9.13, s
3′	2.87, * 2.82, *	2.91, * 2.83, *	2.88, m 2H	2.87, m 2H	2.91, m 2.81, *	2.88, * 2.79, *
5′	3.32, m 3.10, m	3.35, m 3.08, m	3.34, m 3.13, *	3.33, m 3.12, *	3.40, m 3.09, m	3.34, m 3.07, m
6′	3.14, m 2.91, m	3.16, m 2.98, m	3.11, * 2.91, *	3.14, m 2.93, m	3.17, m 3.01, m	3.11, m 2.93, *
9′	6.98, s	6.99, s	7.48, s	7.46, s	7.13, s	6.98, s
12′	6.55, s	6.55, s	6.78, s	7.05, s	7.36, s	6.96, s
14′	1.79, *	1.93, s	1.86, br s	1.86, s	1.84, s	1.82, m
15′	1.67, * 1.03, m	1.76, * 1.49, m	1.74, m 1.09, m	1.73, m 1.07, m	1.71, m 1.07, m	1.70, m 1.05, m
17′	2.61, d, 13.5 1.75, *	2.64, d, 13.6 1.81, m	2.68, * 2.03, *	2.68, d, 13.8 1.89, d, 13.8	2.66, * 1.85, *	2.65, * 1.81, m
18′	0.84, t, 7.3	0.98, d, 6.4	0.90, t, 7.1	0.89, t, 7.2	0.88, t, 7.2	0.86, t, 7.2
19′	1.52, m 1.37, m	3.93, *	1.57, * 1.43, *	1.55, m 1.42, m	1.56, * 1.41, m	1.56, m 1.38, m
20′	1.30, m	1.39, m	1.39, m	1.37, m	1.35, m	1.34, m
21′	3.47, s	3.70, s	3.57, s	3.52, s	3.58, m	3.51, s

(*continued on next page*)

Table 2 (*continued*)

No.	1[a]	2[a]	3[a]	4[b]	5[a]	6[a]
$COOCH_3$'	3.55, s	3.56, s	3.72, s	3.69, s	3.61, s	3.61, s
10′-OCH_3					3.93, s	
11′-OCH_3	3.93, s	3.93, s		3.90, s		3.90, s

[a] ^{1}H recorded at 600 MHz.
[b] at 800 MHz; Overlapped signals were replaced by *.

was already reported on our previous research (Chen et al., 2021) with C3–C10′-C11′-O-C14, which had gave us a misleading in the past until we found the crucial HMBC correlations of H-12′(δ_H 6.55)with C-7′(δ_C 110.0)instead of the H-9' (δ_H 7.48) with C-7' (δ_C 110.0). However, the ROESY correlations (Fig. 3) of H-21/19, H-21/18, H-18/15 and H-19/15 suggested that the relative configuration of unit A was still the same as in conophylline (Kam et al., 1993). Therefore, compound **3** was an aspidosperma–iboga type bisindole alkaloid united by a furan ring named taberdisine C.

Compound **4** possessed a molecular formula of $C_{45}H_{54}N_4O_9$ deduced by a HRESIMS ion peak at m/z 795.3960 $[M + H]^+$ (calcd for $C_{45}H_{55}N_4O_9$ 795.3964). The similar UV and NMR spectrum for **4** and **3** suggested that **4** also possessed an aspidosperma–iboga skeleton. The signals of δ_H 4.97 (dd, J = 7.9, 3.5 Hz, H-14) and δ_H 4.07 (d, J = 3.5 Hz, H-15) in **3** were substituted by epoxy signals of δ_H 3.42 and 3.27 (each d, J = 3.7 Hz) and an additional methoxy in **4**. The newly methoxy was located at C-11′ by the HMBC correlations of δ_H 3.90 (s, OCH_3) and δ_H 7.46 (s, H-9′) with δ_C 155.5 (C-11′). Detailed analyzed of the NMR data deduced this bisindole was connected through C-3/C-10′ connectivity and with was similar to that of conofoline (Kam and Anuradha, 1995; Chen et al., 1998). This was clearly shown by the HMBC correlations (Fig. 4) from the δ_H 7.46 (s, H-9′) to δ_C 53.3 (C-3), 110.5 (C-7′), 137.0 (C-13′), from δ_H 7.05 (s, H-12′) to δ_C 118.0(C-10′), 122.9 (C-8′), and from

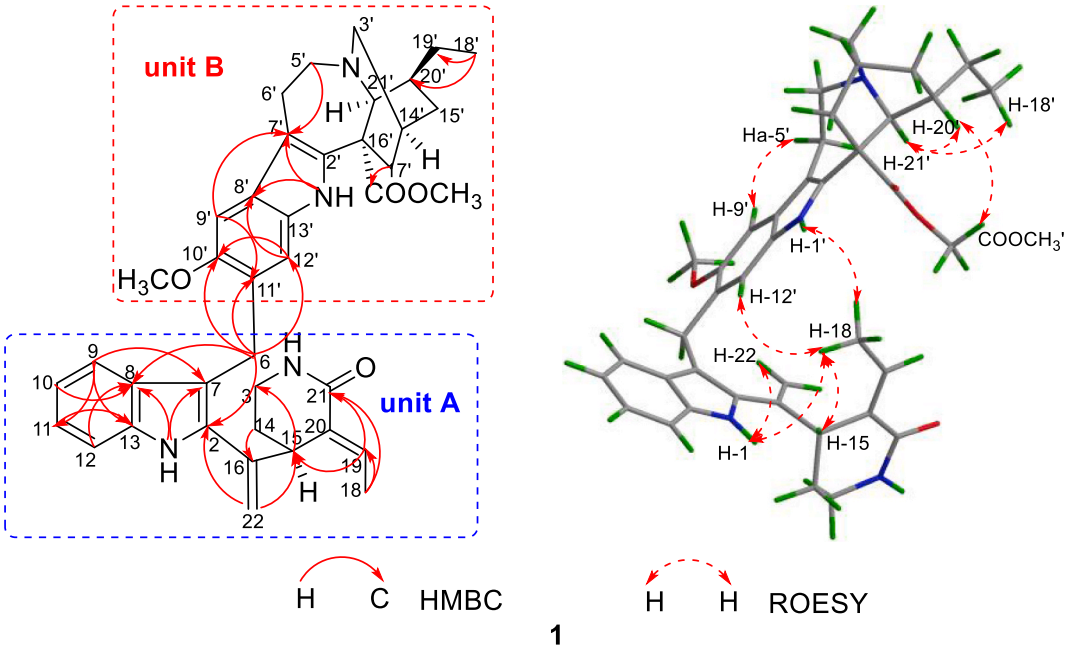

Fig. 2. The key HMBC and ROESY correlations of alkaloid **1**.

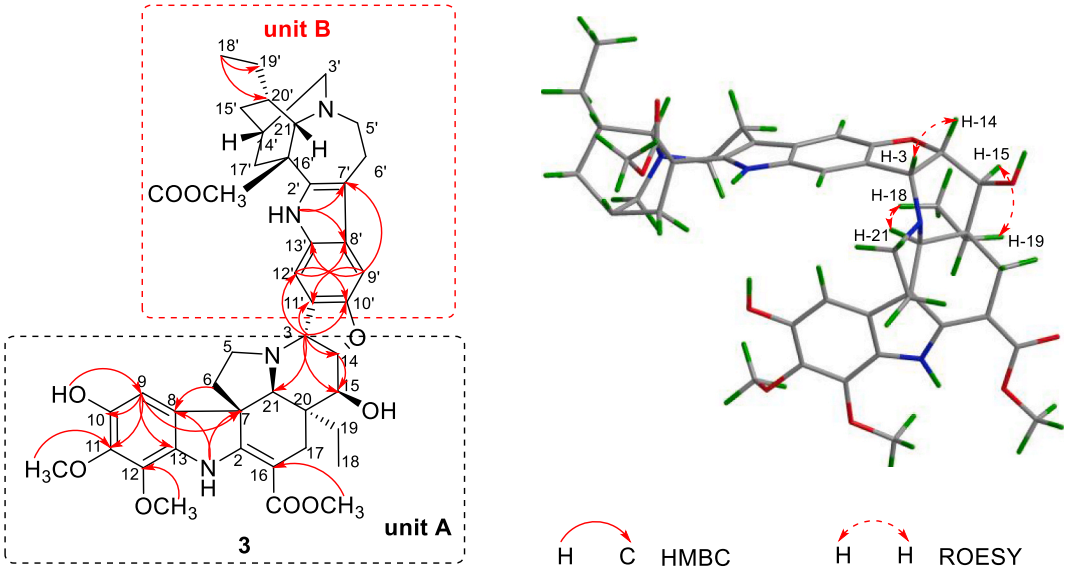

Fig. 3. The key HMBC and ROESY correlations of alkaloid **3**.

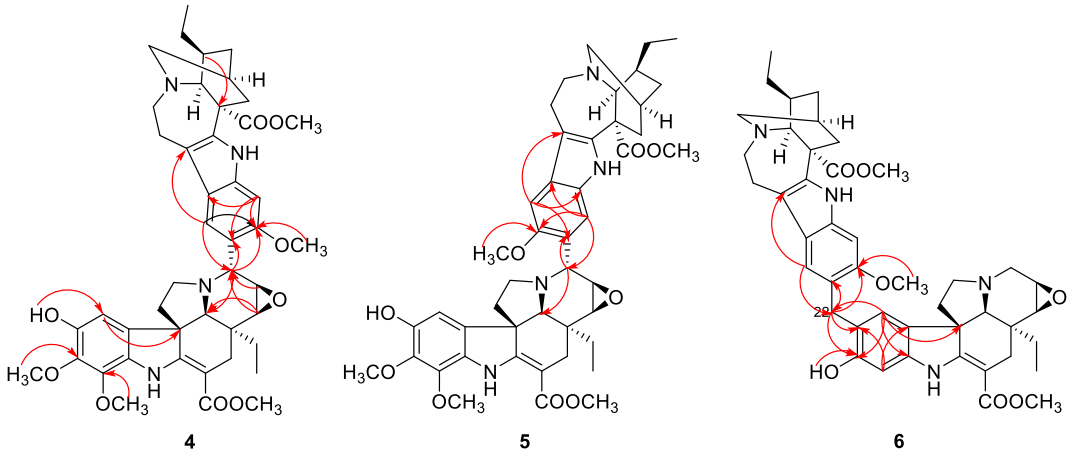

Fig. 4. The key HMBC correlations of alkaloid **4**–**6**.

δ_H 5.01 (s, H-3) to δ_C 118.0 (C-10′), 119.3 (C-9′) and C-11'.

The ROESY correlations of H-3/H-5 and the singlet of H-3 (δ_H 5.01, s) suggested the relative configuration of H-3 was β-orientation, which was the same as that of conofoline and its structural analogues (Kam and Anuradha, 1995; Chen et al., 1998, 2021; Zhang et al., 2018; Yu et al., 2020). Due to the orientation of H-15 and H-14 is in the planar position, and the ROESY correlation of H-18/H-15 both can be detected. Unfortunately, we did not get the single crystal data due to the insufficient quantity of this compound. However, there are still some NMR features that can be found by searching literature. By comparing the data of Pachsiphine and Lochnericine (Kunesch et al., 1980), two typical structures with C-14/15-epoxy in different configurations, when the epoxy structure was in β-orientation, C-19, C-20 and C-21 were δ_C 27.5, 38.1 and 71.8, respectively. While in α-orientation, C-19/C-21 obviously downfiled to δ_C 25.3 and 68.7, respectively, while C-20 upfiled to δ_C 41.9. At the same time, the shielding effect on C-19/18 ethyl side chain also affects the splitting of the two proton signals of C-19 showed one quartet-peak signal. But in β-orientation, the two proton chemical shifts were observed to be two multiple-peak signals. Sum up, the relative configuration of the epoxy ring was confirmed to β-orientation. Then, the structure of **4** was elucidated as shown in Fig. 4 and named taberdisine D.

Compound **5** with $C_{45}H_{55}N_4O_9$ was an isomeric with **4**, as established by HRESIMS m/z = 795.3960 $[M + H]^+$. The ^1H and ^{13}C NMR spectroscopic data of **5** (Tables 1 and 3) indicated the key difference was the substitution position. The methoxy attributed to C-10' (δ_C 153.3) in the iboga unit was supported by HMBC cross-peaks from δ_H 3.93 (s, OCH_3) and δ_H 7.13 (s, H-9′) to δ_C 153.3 (C-10′). The C-3/11′ connectivity between both units was elucidated from the HMBC correlations (Fig. 4) of δ_H 7.13 (s, H-9′) to δ_C 110.5 (C-7′), 120.4 (C-11′), 131.4 (C-13′) and C-10′, from δ_H 7.36 (s, H-12′) to δ_C 128.9 (C-8′), C-10′ and 52.7 (C-3). The similar ROESY correlations (Fig. 5), the key signal of C-3 and coupling constants assigned (H-3/14/15) identical configurations of **5** and **4** and subsequently named **5** as taberdisine E.

Compound **6** possessed a molecular formula of $C_{44}H_{52}N_4O_7$ based on its HRESIMS data at m/z 749.3904 $[M + H]^+$. The UV spectrum of **6** was similar to those of **3**–**5**, suggesting similar structures. Analysis of the ^1H and ^{13}C data of **6** (Tables 2 and 3) also revealed the presence of iboge moiety and tabersonine-β-epoxide moiety. However, there were several notable differences in the NMR data of **6** and **4**. Firstly, in the ^1H NMR spectrum, the signals of 11/12-OCH_3 in **4** were absent in **6**, instead of a newly methylene appeared in **6**. The methylene was a bridge between both units, supported by the HMBC correlations (Fig. 4) from both δ_H 7.08 (s, H-9) and δ_H 6.98 (s, H-9′) to the newly CH_2 (δ_C 31.0). Furthermore, the crucial HMBC cross-peaks of newly methylene (δ_H 3.94, 3.86) to δ_C 124.7 (C-9), 120.1 (C-10), 155.9 (C-11), and 125.8 (C-10′) demonstrated 11-OH in tabersonine unit of **6.** The relative configurations of compound **6** were same to previous alkaloids and named taberdisine F.

Table 3
^{13}C NMR spectroscopic data of alkaloids **4**–**6** in acetone-d_6 (δ in ppm and J in Hz).

No.	4[b]		5[a]		6[a]	
	unit A	unit B	unit A	unit B	unit A	unit B
2/2′	166.4 C	137.3 C	166.4 C	139.4 C	166.7 C	138.3 C
3/3′	53.3 CH	52.5 CH_2	52.7 CH	53.3 CH_2	50.0 CH_2	53.1 CH_2
5/5′	50.1 CH_2	54.2 CH_2	49.8 CH_2	54.3 CH_2	51.6 CH_2	54.3 CH_2
6/6′	43.3 CH_2	22.7 CH_2	43.6 CH_2	22.7 CH_2	45.3 CH_2	22.7 CH_2
7/7′	56.2 C	110.5 C	55.9 C	110.5 C	55.4 C	110.3 C
8/8′	134.8 C	122.9 C	134.6 C	128.9 C	130.0 C	132.0 C
9/9′	105.9 CH	119.3 CH	106.0 CH	100.1 CH	124.7 CH	112.6 CH
10/10′	146.0 C	118.0 C	145.9 C	153.3 C	120.1 C	125.8 C
11/11′	140.4 C	155.5 C	140.4 C	120.4 C	155.9 C	152.5 C
12/12′	138.2 C	94.1 CH	138.2 C	112.6 CH	98.7 C	99.4 CH
13/13′	128.9 C	137.0 C	129.2 C	131.4 C	143.6 C	128.0 C
14/14′	55.5 CH	28.2 CH	55.4 CH	28.3 CH	52.3 CH	28.3 CH
15/15′	56.8 CH	32.9 CH_2	56.3 CH	32.8 CH_2	56.1 CH	32.8 CH_2
16/16′	90.8 C	56.1 C	90.7 C	56.1 C	90.8 C	55.9 C
17/17′	25.2 CH_2	37.0 CH_2	24.4 CH_2	37.1 CH_2	24.6 CH_2	37.0 CH_2
18/18′	7.8 CH_3	11.9 CH_3	7.6 CH_3	11.9 CH_3	7.5 CH_3	11.9 CH_3
19/19′	28.1 CH_2	27.7 CH_2	27.6 CH_2	27.8 CH_2	27.2 CH_2	27.8 CH_2
20/20′	36.9 C	39.5 CH	37.2 C	39.5 CH	37.9 C	39.4 CH
21/21′	63.5 CH	58.4 CH	63.7 CH	57.6 CH	71.7 CH	57.8 CH
22					31.1 CH_2	
$\underline{COOCH_3}$	169.1 C	175.4 C	169.0 C	175.2 C	168.7 C	175.2 C
$COO\underline{CH_3}$	51.0 CH_3	52.6 CH_3	51.0 CH_3	52.6 CH_3	50.9 CH_3	52.5 CH_3
10-OCH_3				56.2 CH_3		
11-OCH_3		55.9 CH_3				56.2 CH_3
11′-OCH_3	61.1 CH_3		61.0 CH_3			
12′-OCH_3	60.8 CH_3		60.8 CH_3			

[a] ^{13}C NMR recorded at 150 MHz.
[b] at 200 MHz.

Newly alkaloids **1**–**6** were evaluated for their inhibition activities on

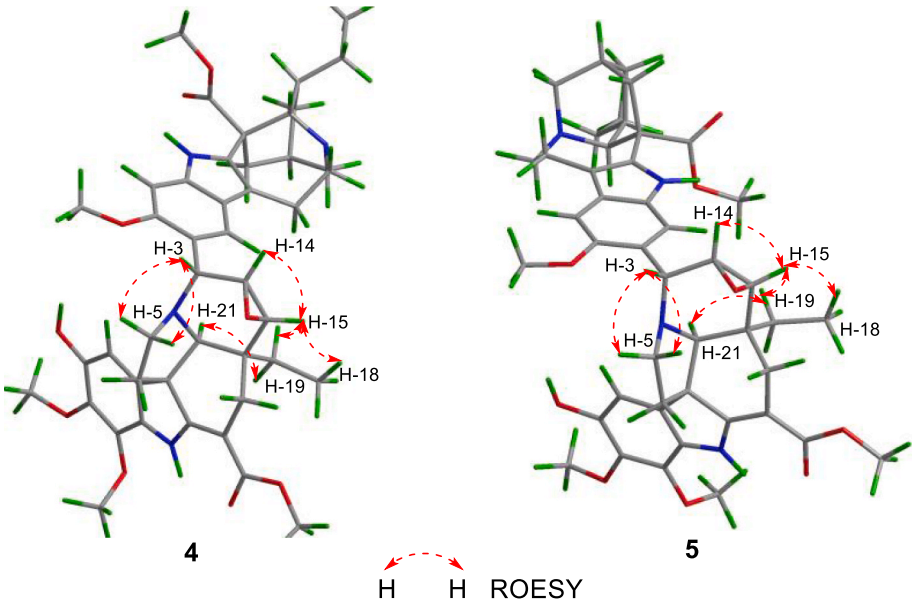

Fig. 5. The key ROESY correlations of alkaloids **4** and **5**.

Sf9 cell. The inhibition activities of all compounds were shown in Table 4, with avermectin as positive control. Among them, alkaloids **1** and **5** showed moderate inhibitory activity with an IC_{50} value of 15.22 and 16.01 μM, compared with that of avermectin with 9.70 μM. The results regarding the **1** and **5** against the *Spodoptera frugiperda* eggs were listed in Table 4 as well. Both compounds displayed the mortality ranging between 12% and 90% at a concentration range of 5–45 μM. Our results demonstrate concentration-dependent mortality with a LD_{90} achieved of **1** and **5** in vivo at concentrations of 39.7 and 40 μM, respectively, compared to avermectin with value of 22.5 ± 1.64 μM.

3. Conclusions

In summary, alkaloids **1** and **2** were the first cases of strychnos–iboga type bisindole alkaloids previously undiscovered. Alkaloid **3**, a new type of aspidosperma–iboga with a furan ring, as well as other three undescribed ones was disclosed from the leaves of *T. divaricata* 'Dwaft'. Bioactive screening disclosed the bisindole alkaloids also acted as insecticide compounds. The occurrence of these bioactive compounds in the leaves suggest a function as defense chemicals against overground organisms.

4. Experimental section

4.1. General experimental procedures

Optical rotations were measured on an Autopol VI, Serial #91058 polarimeter. UV spectra were recorded on a Shimadzu UV-2401PC spectrophotometer. 1D and 2D NMR spectra were acquired on Bruker AV 600 MHz and 800 MHz spectrometers with tetramethylsilane (TMS) as an internal standard. HRESIMS data were recorded on a Shimadzu UPLC-IT-TOF. Column chromatography (CC) was performed on either silica gel (100–200 and 200–300 mesh, Qing-dao Haiyang Chemical Co., Ltd., Qingdao, China) or RP-18 silica gel (50 μm, YMC Chemical Ltd., Japan). Fractions were monitored by TLC on silica gel plates (GF254, Qingdao Haiyang Chemical Co., Ltd., Qingdao, China), and spots were visualized with Dragendorff's reagent. MPLC was performed using a Buchi pump system coupled with RP-18 silica gel-packed glass columns (15 × 230 and 26 × 460 mm), and Sephadex LH-20 (Pharmacia Fine Chemical Co., Ltd., Sweden). HPLC was performed using Waters 1525 pumps coupled with analytical semi-preparative or preparative Sunfire C18 columns (4.6 × 150, and 19 × 250 mm, respectively). The HPLC system employed a Waters 2998 photodiode array detector and a Waters fraction collector III.

Table 4
In vitro cytotoxic activity on *Sf9* cells of alkaloids **1**–**6** and lethal doses of alkaloids **1** and **5** against *Spodoptera frugiperda* eggs in vivo (μM).

No.	Cells	Eggs	
	IC_{50}± SD	IC_{50} ± SD	IC_{90} ± SD
1	15.22 ± 0.22	17.30 ± 1.12	39.7 ± 1.78
5	16.01 ± 1.17	12.0 ± 1.23	40.0 ± 2.36
6	19.87 ± 0.14	/	/
4	33.86 ± 0.65	/	/
2	36.38 ± 1.96	/	/
3	>40	/	/
Avermectin	9.70 ± 0.03	11.2 ± 0.85	22.5 ± 1.64

4.2. Plant material

The leaves of *Tabernaemontana divaricata* 'Dwaft' were collected in November 2018 in Bangkok, Thailand, and identified by Dr. Johann Schinnerl. A voucher specimen (No. Cai20181114) was deposited in Kunming Institute of Botany, Chinese Academy of Sciences.

4.3. Extraction and isolation

Air-dried leaves of *Tabernaemontana divaricata* 'Dwaft' (7.5 kg) were powdered and extracted with MeOH (3−25 L) at room temperature for a week. The extract was partitioned between 0.5% HCl solution and EtOAc, and then the acidic layer was adjusted to pH 8−9 with 25% ammonia solution and subsequently extracted with EtOAc to obtain crude alkaloid extract (68 g). The extract was subjected to column chromatography (CC) over silica gel and eluted with gradient $CHCl_3$/MeOH (1:0–1:1, v/v) to afford five fractions (I ~ V).

Fr. II (25 g) was subjected to C18 MPLC again using MeOH–H_2O (10–100%, v/v) to yield five subfractions (II 1–5). Fr. II-4 (3.5 g) was subjected to MPLC column with MeOH/H_2O (45−65%, v/v) to afford seven parts (II-4-1~7). Part II-4-3 was chromatographed on Sephadex LH-20 (MeOH) to afford four parts (II-4-3-1~4). II-4-3-1 was further purified on the HPLC preparative column with CH_3CN/H_2O (60−80%, v/v) to afford **3** (18.0 mg, 2.4 mg/kg). II-4-3-4 was further purified on

the HPLC preparative column with CH_3CN/H_2O (65−80%, v/v) to afford **6** (1.6 mg, 0.21 mg/kg). Part II-4-4 was chromatographed on Sephadex LH-20 (MeOH) to afford four parts (II-4-4-1∼5). II-4-4-2 was further purified on the HPLC preparative column with CH_3CN/H_2O (60−75%, v/v) to afford **4** (1.1 mg, 0.15 mg/kg) and **5** (10.9 mg, 1.45 mg/kg).

Fr. III (15 g) was subjected to C18 MPLC again using MeOH–H_2O (10–100%, v/v) to yield four subfractions (III-1∼4). Fr. III-4 (2.3 g) was subjected to MPLC column with MeOH/H_2O (5−30%, v/v) to afford six parts (III-4-1∼6). Part III-4-4 was chromatographed on Sephadex LH-20 (MeOH) and further purified on the HPLC preparative column with CH_3CN/H_2O (25−40%, v/v) to afford **2** (2.1 mg, 0.28 mg/kg). Part III-4-6 was purified on the HPLC preparative column with CH_3CN/H_2O (60−75%, v/v) to afford **1** (2.3 mg, 0.31 mg/kg).

4.3.1. Taberdisine A (1)

Amorphous pale powder: [α]25 D - 68.7 (*c* 0.09, MeOH); UV (MeOH) λ max (log ε) nm: 206.0 (3.98), 221.5 (4.03), 298.0 (3.58). For ^{1}H and ^{13}C NMR spectroscopic data (acetone-d_6), see Tables 1 and 2; HRESIMS *m/z* 647.3594 $[M + H]^+$ (calcd for $C_{40}H_{47}N_4O_4$ 647.3592).

4.3.2. Taberdisine B (2)

Amorphous white powder: [α]25 D - 53.4 (*c* 0.13, MeOH); UV (MeOH) λ max (log ε) nm: 204.5 (3.91), 221.5 (3.97), 298.0 (3.53). For ^{1}H and ^{13}C NMR spectroscopic data (acetone-d_6), see Tables 1 and 2; HRESIMS *m/z* 663.3543 $[M + H]^+$ (calcd for $C_{40}H_{47}N_4O_5$ 663.3541).

4.3.3. Taberdisine C (3)

Amorphous white powder: [α]25 D - 32.3 (*c* 0.06, MeOH); UV (MeOH) λ max (log ε) nm: 204.5 (3.89), 219.0 (3.84), 304.5 (3.52), 336.5 (3.27). For ^{1}H and ^{13}C NMR spectroscopic data (acetone-d_6), see Tables 1 and 2; HRESIMS *m/z* 781.3803 [M + H]+(calcd for $C_{44}H_{53}N_4O_9$ 781.3807).

4.3.4. Taberdisine D (4)

Amorphous white powder: [α]25 D - 198.8 (*c* 0.12, MeOH); UV (MeOH) λ max (log ε) nm: 211.0 (3.71), 225.5 (3.74), 304.5 (3.37), 336.5 (3.14). For ^{1}H and ^{13}C NMR spectroscopic data (acetone-d_6), see Tables 2 and 3; HRESIMS *m/z* 795.3960 $[M + H]^+$ (calcd for $C_{45}H_{55}N_4O_9$ 795.3964).

4.3.5. Taberdisine E (5)

Amorphous white powder; [α]25 D - 284.5 (*c* 0.12, MeOH); UV (MeOH) λ max (log ε) nm: 211.0 (3.80), 225.5 (3.82), 302.0 (3.56), 339.0 (3.29). For ^{1}H and ^{13}C NMR spectroscopic data (acetone-d_6), see Tables 2 and 3; HRESIMS *m/z* 795.3968 $[M + H]^+$ (calcd for $C_{45}H_{54}N_4O_9$ 795.3964).

4.3.6. Taberdisine F (6)

Amorphous white powder: [α]25 D - 142.7 (*c* 0.07, MeOH); UV (MeOH) λ max (log ε) nm: 206.0 (3.79), 217.5 (3.78), 304.5 (3.44), 328.5 (3.35). For ^{1}H and ^{13}C NMR spectroscopic data (acetone-d_6), see Tables 2 and 3; HRESIMS *m/z* 749.3904 $[M + H]^+$ (calcd for $C_{44}H_{53}N_4O_7$ 749.3909).

4.4. Bioactivity

In vitro cytotoxicity of alkaloids **1**−**6** and avermectin on *Sf9* cells were assessed via MTT assay. Cytotoxic effects were determined using 96-well flat-bottomed plastic microplates. Cells with a density of 5000 cells per millilitre (100 μL) were seeded into each well. After overnight incubation, the cells were exposed to all six compounds with various concentrations (5, 10, 20, 40 and 80 μM) for 72 h. The cell viability was analyzed by the MTT colorimetric method by measuring the absorbance at 490 nm using the CellTiter 96 AQueous One Solution Cell Proliferation Assay kit (Promega, USA) and an Infinite M200 Pro (Tecan, Austria) microplate reader, and calculated as the percent of absorbance in the control (medium treated cells). IC_{50} values were calculated using Reed-Muench method.

Different concentrations (3, 15, and 45 μg/mL) of alkaloids **1**, **5** and Avermectin were prepared by diluting 0.01% Tween-80 in 0.5% aqueous acetone. The plastic trays were filled with the required concentration to half of its capacity. The control group only contained aqueous acetone (0.5%) with 0.01% Tween-80. To determine the ovicidal activity of the **1** and **5** using the same concentrations as mentioned above, small plastic trays (250 mL) were used for the assay. Freshly laid eggs of *Spodoptera frugiperda* were collected on filter paper. A disinfected blade was used to cut the area of filter paper with 30 eggs. Wet filter papers were air-dried; later, these filter papers with eggs were dipped and placed on a plastic tray containing the relevant treatment (125 mL). Aqueous acetone (0.5%) containing 0.01% Tween-80 was set as control. Each treatment was replicated three times. The date regarding egg hatching was recorded after 24 h of each treatment up until 5 days (Shoukat et al., 2020).

CRediT authorship contribution statement

Jing Chen: Writing – original draft, Visualization, Software, Investigation, Formal analysis, Data curation. **Sumet Kongkiatpaiboon:** Resources, Funding acquisition. **Xiang-Hai Cai:** Writing – review & editing, Supervision, Resources, Project administration, Methodology, Funding acquisition, Conceptualization.

Declaration of competing interest

The authors declare that they have no known competing financial interests or personal relationships that could have appeared to influence the work reported in this paper

Data availability

Data will be made available on request.

Acknowledgments

This work was supported by the Applied Basic Research Key Project of Yunnan (202201AS070050), Biological Medicine Special Project of Yunnan (202202AA100005), Revitalizing Yunnan Talents, and Bualuang ASEAN Chair Professor Research Grand.

Appendix A. Supplementary data

Supplementary data to this article can be found online at https://doi.org/10.1016/j.phytochem.2024.114075.

References

Agwada, V.C., Morita, Y., Renner, U., Hesse, M., Schmid, H., 1975. Alkaloids. 155. Alkaloids from *Gabunia eglandulosa* stapf. Helv. Chim. Acta 58, 1001–1016. https://doi.org/10.1002/hlca.19750580405.

Albinsson, B., Norden, B., 1992. Excited-state properties of the indole chromophore: electronic transition moment directions from linear dichroism measurements: effect of methyl and methoxy substituents. J. Phys. Chem. 96, 6204–6212. https://doi.org/10.1021/j100194a023.

Arens, H., Borbe, H.O., Ulbrich, B., Stockigt, J., 1982. Detection of pericine, a new CNS-active indole alkaloid from *Picralima nitida* cell suspension culture by opiate receptor binding studies. Planta Med. 46, 210–214. https://doi.org/10.1055/s-2007-971216.

Chaturvedula, V.S.P., Sprague, S., Schilling, J.K., Kingston, D.G.I., 2003. New cytotoxic indole alkaloids from *Tabernaemontana calcarea* from the Madagascar rainforest. J. Nat. Prod. (Lloydia) 66, 528–531. https://doi.org/10.1021/np020548e.

Chen, W., Anuradha, S., Kam, T.S., 1998. Crystal structure of conofoline, $C_{43}H_{54}N_4O_8$. Z. Krist. - New Cryst. St. 213, 183–184. https://doi.org/10.1524/ncrs.1998.213.14.183.

Chen, J., Yu, Y., Wu, J., Bao, M.F., Kongkiatpaiboon, S., Schinnerl, J., Cai, X.H., 2021. Trimeric and dimeric Aspidosperma-type alkaloids from leaves of *Tabernaemontana*

divaricata 'Dwaft'. Bioorg. Chem. 116, 105314 https://doi.org/10.1016/j.bioorg.2021.105314.

Duke, S.O., Evidente, A., Vurro, M., 2019. Natural products in pest management: innovative approaches for increasing their use. Pest Manag. Sci. 75, 2299–2300. https://doi.org/10.1002/ps.5552.

Dwivedi, S.C., Venugopalan, S., 2002. Olfactory response of *Callosobruchus chinensis* (Linn.) to the odours of six plant extracts. J. Adv. Zool. 23, 77–79. This article has no DIO.

Fouche, G., Adenubi, O.T., Leboho, T., McGaw, L.J., Naidoo, V., Wellington, K.W., Eloff, J.N., 2019. Acaricidal activity of the aqueous and hydroethanolic extracts of 15 South African plants against *Rhipicephalus turanicus* and their toxicity on human liver and kidney cells. Onderstepoort J. Vet. 86, e1–e7. https://doi.org/10.4102/ojvr.v86i1.1665.

Ganesan, P., Samuel, R., Mutheeswaran, S., Pandikumar, P., Reegan, A.D., Aremu, A.O., Ignacimuthu, S., 2023. Phytocompounds for mosquito larvicidal activity and their modes of action: a review. S AFR J BOT 152, 19–49. https://doi.org/10.1016/j.sajb.2022.11.028.

Govindarajan, M., Mathivanan, T., Elumalai, K., Krishnappa, K., Anandan, A., 2011a. Mosquito larvicidal, ovicidal, and repellent properties of botanical extracts against *Anopheles stephensi, Aedes aegypti*, and *Culex quinquefasciatus* (Diptera: Culicidae). Parasitol. Res. 109, 353–367. https://doi.org/10.1007/s00436-011-2263-1.

Govindarajan, M., Mathivanan, T., Elumalai, K., Krishnappa, K., Anandan, A., 2011b. Ovicidal and repellent activities of botanical extracts against *Culex quinquefasciatus, Aedes aegypti* and *Anopheles stephensi* (Diptera: Culicidae). APJTB 1, 43–48. https://doi.org/10.1016/S2221-1691(11)60066-X.

Govindarajan, M., Sivakumar, R., Amsath, A., Niraimathi, S., 2012. Larvicidal efficacy of botanical extracts against two important vector mosquitoes. Eur. Rev. for Med. Phamaco. 16, 386–392. This article has no DIO.

Gunasekera, S.P., Cordell, G., Farnsworth, N.R., 1980. Anticancer indole alkaloids of *Ervatamia heyneana*. Phytochemistry 19, 1213–1218. https://doi.org/10.1016/0031-9422(80)83086-X.

Hillary, V.E., Ceasar, S.A., Ignacimuthu, S., 2024. Efficacy of plant products in controlling disease vector mosquitoes, a review. Entomol. Exp. Appl. 172, 195–214. https://doi.org/10.1111/eea.13401.

Kam, T.S., Anuradha, S., 1995. Alkaloids from *Tabernaemontana divaricata*. Phytochemistry 40, 313–316. https://doi.org/10.1016/0031-9422(95)00266-A.

Kam, T.S., Sim, K.M., 2002. Five new iboga alkaloids from *Tabernaemontana corymbosa*. J. Nat. Prod. (Lloydia) 65, 669–672. https://doi.org/10.1021/np0105432.

Kam, T.S., Loh, K.Y., Wei, C., 1993. Conophylline and conophyllidine - new dimeric alkaloids from *Tabernaemontana divaricata*. J. Nat. Prod. (Lloydia) 56, 1865–1871. https://doi.org/10.1021/np50101a001.

Kam, T.S., Sim, K.M., Koyano, T., Toyoshima, M., Hayashi, M., Komiyama, K., 1998. Conodiparines A-D, new bisindoles from Tabernaemontana. Reversal of vincristine-resistance with cultured cells. Bioorg. Med. Chem. Lett. 8, 1693–1696. https://doi.org/10.1016/S0960-894X(98)00294-7.

Kam, T.S., Pang, H.S., Lim, T.M., 2003. Biologically active indole and bisindole alkaloids from *Tabernaemontana divaricata*. Org. Biomol. Chem. 1, 1292–1297. https://doi.org/10.1039/B301167D.

Kobayashi, J., Shimamoto, M.S., S, Shigemori, H., Ishiyama, H., Ohsaki, A., 2002. Subincanadines A-C, novel quaternary indole alkaloids from *Aspidosperma subincanum*. J. Org. Chem. 67, 6449–6455. https://doi.org/10.1021/jo025854b.

Kunesch, N., Cavé, A., Hagaman, E.W., Wenkert, E., 1980. Dimeric indoline alkaloids of a new biphenyl type. Tetrahedron Lett. 21, 1727–1730. https://doi.org/10.1016/S0040-4039(00)77821-X.

Lim, K.H., Kam, T.S., 2007. Secoleuconoxine and oxopericine derivatives from Kopsia. Helv. Chim. Acta 90, 31–35. https://doi.org/10.1002/hlca.200790018.

Mathivanan, T., Govindarajan, M., Govindarajan, M., Elumalai, K., Krishnappa, K., Ananthan, A., 2013. Mosquito larvicidal and phytochemical properties of *Ervatamia coronaria* stapf. (Family: Apocynaceae). J. Vector. Dis. 47, 178–180. This article has no DOI itself.

Perera, P., Vanbeek, T.A., Verpoorte, R., 1983. Tertiary indole alkaloids from leaves of *Tabernaemontana dichotoma*. 2. dichomine, a novel type of Iboga alkaloid. Planta Med. 47, 148–150. https://doi.org/10.1055/s-2007-969974.

Sharma, P., Cordell, G.A., 1988. Heyneanine hydroxyindolenine, a new indole alkaloid from *Ervatamia coronaria* var. plena. J. Na. Prod 51, 528–531. https://doi.org/10.1021/np50057a012.

Shoukat, R.F., Shakeel, M., Rizvi, S.A.H., Zafar, J., Zhang, Y., Freed, S., Xu, X., Jin, F., 2020. Larvicidal, Ovicidal, synergistic, and repellent activities of *Sophora alopecuroides* and its dominant constituents against *Aedes albopictus*. Insects 11, 246. https://doi.org/10.3390/insects11040246.

Van Beek, T.A., Verpoorte, R., Svendsen, A.B., 1984. Isolation and synthesis of vobparicine, a novel type dimeric indole alkaloid. Tetrahedron Lett. 25, 2057–2060. https://doi.org/10.1016/S0040-4039(01)90112-1.

Yu, Y., Zhao, S.-M., Bao, M.-F., Cai, X.-H., 2020. An Aspidosperma-type alkaloid dimer from Tabernaemontana bovina as a candidate for the inhibition of microglial activation. Journal 7, 1365–1373. https://doi.org/10.1039/d0qo00296h.

Zhang, B.J., Lu, J.S., Bao, M.F., Zhong, X.H., Ni, L., Wu, J., Cai, X.H., 2018. Bisindole alkaloids from Tabernaemontana corymbosa. Journal 152, 125–133. https://doi.org/10.1016/j.phytochem.2018.04.020.